Model Order Reduction of 3D Electro-Thermal Model for a Novel Micromachined Hotplate Gas Sensor

Tamara Bechtold[(1)], Jürgen Hildenbrand[(1)], Jürgen Wöllenstein[(2)] and Jan G. Korvink[(1)]
[(1)]IMTEK, University of Freiburg, Georges Köhler Allee 103, 79110 Freiburg, Germany,
E-mail:bechtold@imtek.de
[(2)]Institute for Physical Measurement Techniques, Heidenhofstr. 8, 79110 Freiburg, Germany

Abstract

In this paper we present an automatic, Arnoldi-based model order reduction of a 3D electro-thermal model for a novel sensor device. Model order reduction is essential for achieving quickly evaluable, yet still accurate macromodel of the device, needed for system-level simulation. We present below numerical simulation results of the full-scale finite element model and the compact-reduced order model, and show how the nonlinearities in the input function can be treated even with linear reduction algorithm.

1. Introduction

Presented device is a novel metal oxide low power microhotplate gas sensor array [1]. In order to simultaneously assure a robust design and excellent thermal isolation of the membrane from the surrounding wafer, the silicon microhotplate platform is supported by glass pillars emanating from a glass cap above the silicon wafer Fig. 1. Glass (Pyrex #7740) was chosen for its low thermal conductivity and anodic bondability to silicon.

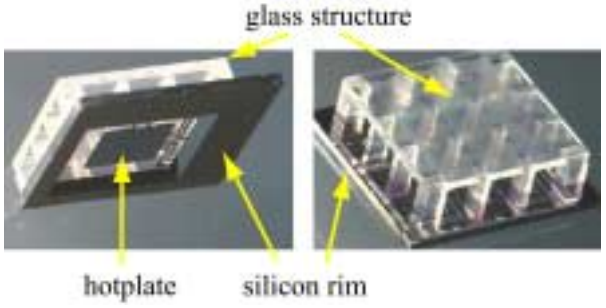

Fig. 1 Micromashined metal oxide gas sensor array; Bottom view (left), top view (right).

Designing a microhotplate gas sensor thermal management is of crucial importance. Hereby several points have to be considered, such as the homogenous temperature distribution over the gas sensitive regions, and the good thermal decoupling between hotplate and silicon rim. The quality of this thermal decoupling correlates with the power consumption and in conjunction with the thermal mass of the hotplate with the heating time. Due to the glass structure, direct measurements of the temperature distribution on the sensor platform are not possible. Thus modelling and simulation are the only way to evaluate these parameters.

The heat conduction within the hotplate is described through the following governing equations:

$$\nabla \bullet (\kappa \nabla T) + Q - \rho c \frac{\partial T}{\partial t} = 0, Q = \frac{\boldsymbol{j}^2}{\sigma} \qquad (1)$$

where κ is the thermal conductivity, C_p is the specific heat capacity, ρ is the mass density, T is the temperature distribution, Q is the heat generation rate (Joule heating is taken as the dominant heating mechanism), $\boldsymbol{j}$ is the spatially varying electric current density vector and σ is the specific electric conductivity. Assuming that the heat generation Q is uniformly distributed within the heating area (lumped resistor), and that the system matrices are temperature independent around the working point, the finite element based spatial discretization of (1) leads to a large linear ODEs system of the form:

$$\begin{aligned} C\dot{\boldsymbol{T}} + K\boldsymbol{T} &= \boldsymbol{F}P(t) \\ y &= E^T \cdot T \end{aligned} \qquad (2)$$

where $K, C \in R^{nxn}$ are the global heat conductivity and heat capacity matrix, $\boldsymbol{T}(t), \boldsymbol{F}, E \in R^n$ are the temperature (state), the load and the output vector respectively and $n = 73955$ is the dimension of the system. The electric power $P(t)$, which is assumed to be completely transformed into the heating power is the input to the system. As the above number of equations is too high for subsequent system-level simulation, model reduction is necessary. In the following we present numerical simulation results of the finite element model which are in good agreement with the results of a reduced model. Furthermore, we explain in more details how the resistor's dependence on temperature was considered. In chapter 2 and 3 the finite element model of the device and the model order reduction via Arnoldi algorithm explained. Chapter 4 shows in detail how this linear reduction algorithm can be used for limited nonlinear systems. In chapter 5 and 6 the results and conclusion are presented.

2. Finite Element Model

The finite element (FE) model contains the three main components silicon rim, silicon hotplates and glass structure as well as the platinum heater and the thermal cou-

pling between hotplate and silicon rim via the platinum electrodes and the dielectric passivism layer. The thermal coupling via the ambient air was considered in the model too. Fig. 2 shows the FE model without the ambient air.

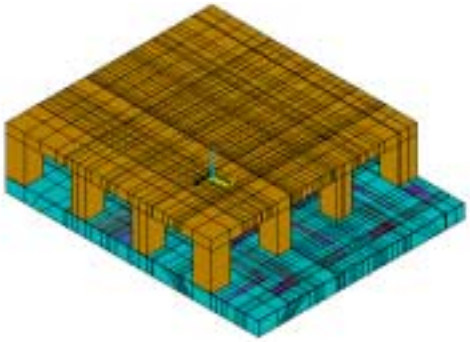

Fig. 2 Finite element model of the gas sensor.

Numerical simulation result of the temperature distribution over the chip and on the hotplate are shown in Fig. 3 and Fig. 4.

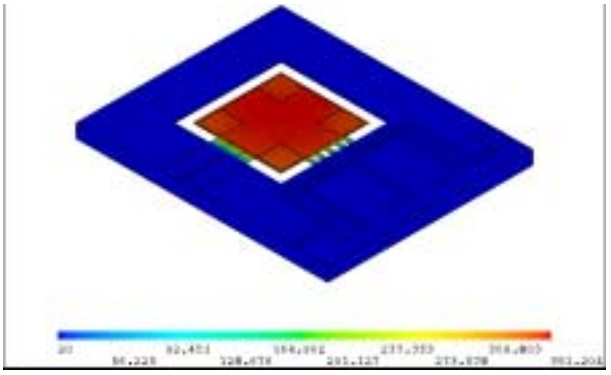

Fig. 3 Temperature distribution over the chip for applied constant heating power of 340mW.

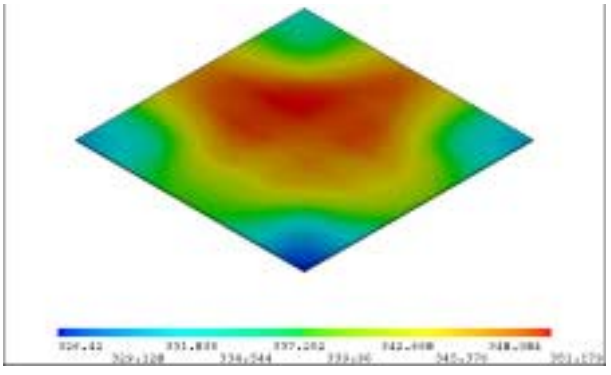

Fig. 4 Temperature distribution on the hotplate for applied constant heating power of 340mW.

Main results of the simulations are, that the heater and the electrodes do not essentially influence the maximal temperature of the hotplate, but rather its temperature distribution.

It is also important to mention, that for this device a dynamic thermal behavior is of special interest when temperature pulsed gas measurement is required. Such measurement has two main advantages: First, more data information can be received, since measurements are done at different operation temperatures and second, the energy consume is lower.

3. Dynamic Compact Thermal Modeling via Moment Matching

In the last years many papers have been devoted to the generation of dynamic compact thermal models. An extensive review can be found in [2]. A large set of approaches is based on fitting an RC ladder network on the observed system response using a suitable optimization algorithm [3]. Such a non-automatic approach requires the designer to choose the right number and position of the RC ladder elements without strict guidelines, and to perform a time-consuming parametrization and simulation of the full-scale model. Another, more automatic way to proceed, is to perform mathematical order reduction of the ODE-system (2). Into this group belongs, for example a commercially available modal reduction approach [4], based on neglecting a number of non-relevant eigenvalues. The main disadvantage of this approach is that there is again no guideline how to chose the relevant modes. A related approach that we propose here is a moment matching technique via Arnoldi algorithm [5], which can be described as follows.

Goal is to transform the equation system (2) into the similar system:

$$\begin{aligned} C_r \dot{\boldsymbol{T}}_{\boldsymbol{r}} + K_r \boldsymbol{T}_{\boldsymbol{r}} &= \boldsymbol{F}_{\boldsymbol{r}} P(t) \\ y_r &= E_r^{\,T} \cdot T_r \end{aligned} \tag{3}$$

with much smaller dimension $r \ll n$. Here T_r can be seen as a projection of the n-dimensional temperature vector to r-dimensional subspace, subjected to some error ε:

$$\boldsymbol{T} = V \cdot \boldsymbol{T}_{\boldsymbol{r}} + \varepsilon, \boldsymbol{T}_{\boldsymbol{r}} \in R^r, r \ll n \tag{4}$$

and $y_r = E_r^{\,T} \cdot T_r$ is those linear combination of the reduced states which corresponds to the required states y in equation (2).

The matrix V in (4) is composed from r n-dimensional vectors that form a basis for the reduced subspace. When the subspace is found the whole equation (2) is projected onto it (by applying (4) and then multiplying (2) from the left side by V^T), and this projection process produces a reduced order system (3) according to the Pade or Pade-type approximation [6]:

$$C_r = V^T C V; K_r = V^T K V; \boldsymbol{F}_r = V^T \boldsymbol{F}; E_r = V^T E \quad (5)$$

It can be shown that the transfer functions of the systems (2) and (3) when developed into Maclaurin expansion:

$$\{G(s)\} = -\sum_{i=0}^{\infty} \{m\}_i s^i \quad (6)$$

where $\{m\}_i = E^T(-C^{-1}K)^{-(i+1)}C^{-1}F$ is called the i*th* moment, match the first r moments.

For the large linear systems a transformation matrix V can be effectively computed as an orthogonal basis for the Krylov subspace of the dimension *r*.

$$K_r\{A, \boldsymbol{b}\} = span\{\boldsymbol{b}, A\boldsymbol{b}, \ldots, A^{r-1}\boldsymbol{b}\} \quad (7)$$

with $A = -K^{-1}C$, $\boldsymbol{b} = -K^{-1}\boldsymbol{F}$. This matrix is a direct output of Arnoldi algorithm. Furthermore, in [5] we have shown, that for the linear (in sense of temperature independent system matrices) dynamic thermal models, the Single-Input-Single-Output setup for the Arnoldi algorithm is sufficient to approximate not only a single output response but also the transient thermal response in all the finite element nodes of the device. Hence, for thermal problems it functions even when E is a unit matrix of the dimension n. Our new software tool *mor4ansys* [7] constructs the equation system (2) directly out of ANSYS binary element matrix file, and performs Arnoldi algorithm (as described above) to create a low dimensional system.

4. Nonlinearities in the Input Function

By designing a heater it is necessary to calculate it's electrical resistivity R. Under the assumption that the electric power is completely transformed into the heating power we can set:

$$P(t) = \frac{U^2(t)}{R} \quad (8)$$

where $U(t)$ is applied voltage. Hereby, the heaters resistivity is a function of temperature itself:

$$R = R(T) = R_0 \cdot (1 + \alpha T + \beta T^2 + \ldots) \quad (9)$$

where R_0 is resistivity at $0°C$, and α and β are the temperature coefficients. For a platinum sensor's heater it is enough to assume linear temperature dependence in range from $0°C$ to $500°C$, i. e. β can be neglected.
In order to be able to control heaters resistivity, and so the temperature of the hotplate, equation (9) must be taken into account. Hence, a linear equation system (2) changes into the weak nonlinear system:

$$\begin{aligned} C\dot{\boldsymbol{T}} + K\boldsymbol{T} &= \boldsymbol{F}P(t, T) = \boldsymbol{F} \cdot \frac{U^2(t)}{R(T)} \\ y &= E^T \cdot T \end{aligned} \quad (10)$$

Dependence of the heaters resistivity on temperature and consequent dependence of the heating power on temperature are shown in Fig. 5 and Fig. 6.

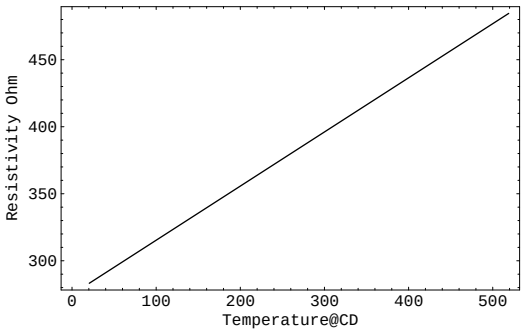

Fig. 5 Heaters resistivity as a function of temperature.

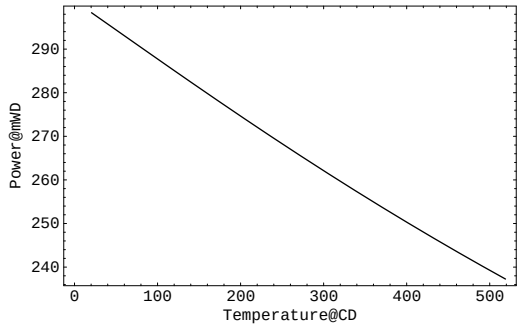

Fig. 6 Heating power as a function of temperature, measured for the constant input voltage of 14V.

The main question is now: can we reduce the equation system (10) by using the same linear Arnoldi, as described above? The answer is yes [8], because due to the fact, that the nonlinear input term $P(t, T)$ doesn't take part in the model order reduction, it is possible to overtake it into the reduced system, which will then be of the form:

$$\begin{aligned} C_r\dot{\boldsymbol{T}}_r + K_r\boldsymbol{T}_r &= \boldsymbol{F}_r P(t, T) \\ y_r &= E_r^T \cdot T_r \end{aligned} \quad (11)$$

or, by applying a projection (4):

$$\begin{aligned} V^T C V\dot{\boldsymbol{T}}_r + V^T K V\boldsymbol{T}_r &= V^T \boldsymbol{F}P(t, V \cdot T_r) \\ y_r &= E^T V T_r \end{aligned} \quad (12)$$

The implementation of (10) and (12) will be discussed in the next chapter.

5. Results

5.1 Linear Model

In Fig. 7 and Fig. 8 the transient solution and error between the full-scale and the reduced model in case of constant heating power of 340mW are shown. In this case,

a purely thermal system was implemented (using heat generation rate as a load in ANSYS7.0) and reduced. Hence, the equations (2) and (3) were integrated for $P(t) = 340mW$. The frequency responses of the original model and three reduced order models are shown in Fig. 9. It testifies a well agreement between the transfer function of the full-scale and of the reduced model in low-frequency domain, as granted through the development around $s = 0$ in equation (6).

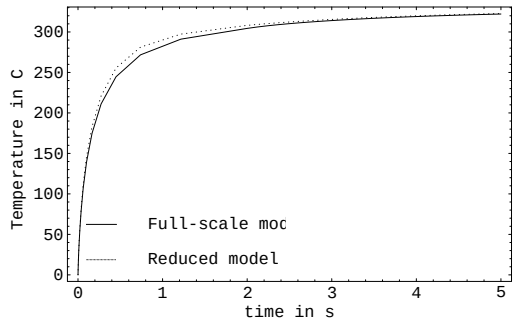

Fig. 7 Solution of the full 73. 955 order system and of the reduced order-50 system in a central hotplate node, for constant heating power of 340mW.

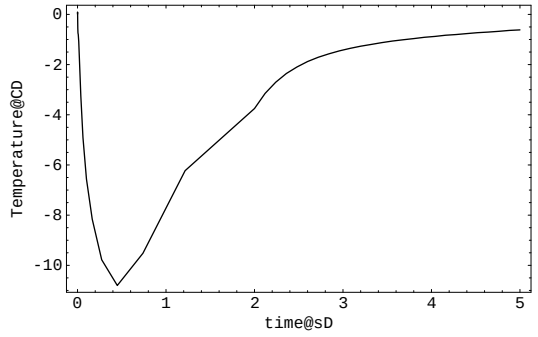

Fig. 8 Difference between the full-scale and the reduced solution, corresponding to results in Fig. 7.

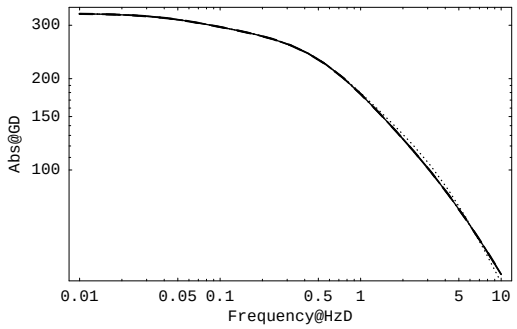

Fig. 9 Frequency response.

Lastly, through model order reduction the computation time was reduced by a factor of 10, including the time needed for the very reduction of the equation system Fig. 10.

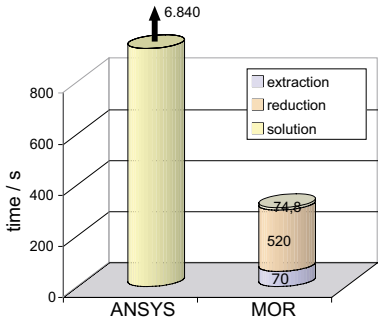

Fig. 10 Computational times for a full-scale model (ANSYS) and the reduced model (MOR) showing a decrease by a factor of 10 (computation done with Ultra SPARC 10).

5.2 Nonlinear Model

In Fig. 11 and Fig. 12 the transient solution and error between the full-scale and the reduced model in case of temperature dependant heating power (according to the Fig. 6) are shown. Also in this case, a purely thermal system was implemented (using the nonlinear heat generation rate as a table load in ANSYS7.0) and reduced. A temperature of the meander was however approximated through a single node temperature, say T_N, so that the heating power could be expressed as:

$$P(t, T) = P(T_N(t)) \tag{13}$$

Hence, the equations (10) and (12) were integrated, by using those linear combination of reduced states T_r in (12), which corresponds to T_N.

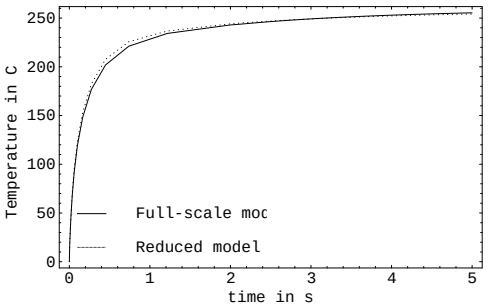

Fig. 11 Solution of the full 73. 955 order system and of the reduced order-50 system in a central hotplate node, for temperature dependant heating power according to Fig. 6.

As expected, the reached steady-state of nonlinear thermal model differs from the one for linear thermal model.

5.3 HDL Model

Nonlinearities in the input function can further be treated within a system level model. Fig. 13 shows a struc-

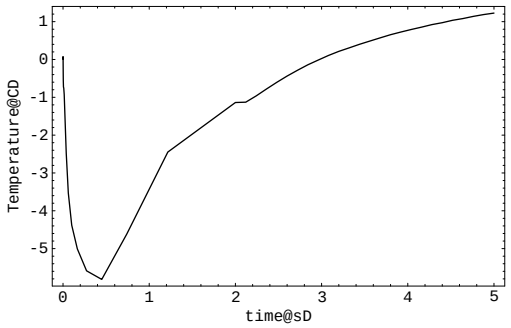

Fig. 12 Difference between the full-scale and the reduced solution, corresponding to results in Fig. 11.

ture of a HDL model for gas sensor. It contains a reduced order model in a form of an equation system (this is supported by e. g. SABER simulator) with a back coupled heaters resistance dependant again on a particular linear combination of reduced states T_r. Basically, there is no difference between this implementation and the implementation in chapter 5.2.

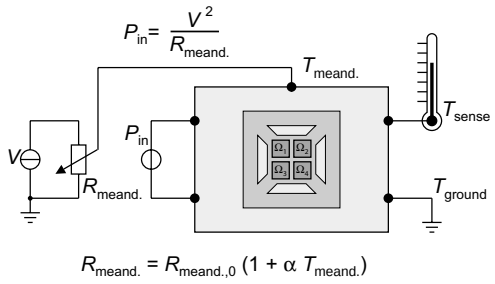

Fig. 13 HDL model structure containing linear reduced model and back coupled temperature dependant heater.

6. Conclusion

We have shown that by means of model order reduction via Arnoldi an accurate dynamic compact thermal model of the microhotplate gas sensor can be generated. It has been further shown, that this linear reduction algorithm can be well used for limited nonlinear systems, in case when the nonlinearities appear only within the input function. For a gas sensor, this the case with temperature dependence of the heaters resistivity or heating power. The nonlinearities within the input function can also be treated during the system level simulation.

7. Acknowledgments

The Authors would like to thank Dr. Evgenii Rudnyi for having used his software tool *mor4ansys*. This work was partially funded by the EU through the project GlassGas-II (IST-99-19003) led by Dr. C. Cane and partially by an operating grant of the University of Freiburg.

8. References

[1] J. Wöllenstein, H. Böttner, J. A. Plaza, C. Cane, Y. Min, H. L. Tuller, "A novel single chip thin film metal oxide array", *Sensors and Actuators B: Chemical* **93** (1-3), pp. 350-355, (2003).

[2] M. N. Sabry, "Dynamic Compact Thermal Models Used for Electronic Design: A Review of Reacent Progress", *Proz. IPACK03*, (2003).

[3] M. renc, V. Szekely, "Dynamic Thermal Multiport Modeling of IC Packages", *IEEE Trans. CPT*, **24**, pp. 596-604 (2001).

[4] ANSYS Release 5.6 User Manuals-Theorie Manual, (1999).

[5] T. Bechtold, E. B. Rudnyi, J. G. Korvink, Automatic Generation of Compact Electro-Thermal Models for Semiconductor Devices, *IEICE Trans. on Electron.*, E86-C, **3**, pp. 459-465, (2003).

[6] E. B. Rudnyi, J. G. Korvink, Review: Automatic Model Reduction for Transient Simulation of MEMS-based Devices, *Sensors Update*, **11**, pp. 3-33, (2002).

[7] T. Bechtold, Evgenii B. Rudnyi, J. G. Korvink, "Efficient modeling and simulation of 3D electro-thermal model for a pyrotechnical microthruster", Proz. PowerMEMS2003.

[8] Z. Bai et. al., "New Numerical Techniques and Tools in SUGAR for 3D MEMS Simulation", *Proz. MSM2001*, pp. 31-34 (2001).